

# Probe Mobility in Native Phosphocaseinate Suspensions and in a Concentrated Rennet Gel: Effects of Probe Flexibility and Size

Souad Salami,<sup>†,‡</sup> Corinne Rondeau-Mouro,<sup>†,‡</sup> John van Duynhoven,<sup>§,||</sup> and François Mariette<sup>\*,†,‡</sup>

<sup>†</sup>Irstea, UR TERE, 17 avenue de Cucillé, CS 64427, F-35044 Rennes, France

<sup>‡</sup>Université européenne de Bretagne, 5 Boulevard Laënnec, 35000 Rennes, France

<sup>§</sup>Unilever R&D, Olivier van Noortlaan 120, P.O. Box 3130AC, Vlaardingen, The Netherlands

<sup>||</sup>Laboratory of Biophysics, Wageningen University, Dreijenlaan 3, 6703HA, Wageningen, The Netherlands

## S Supporting Information

**ABSTRACT:** Pulsed field gradient nuclear magnetic resonance and proton nuclear magnetic resonance relaxometry were used to study the self-diffusion coefficients and molecular dynamics of linear (PEGs) and spherical probes (dendrimers) in native phosphocaseinate suspensions and in a concentrated rennet gel. It was shown that both the size and the shape of the diffusing molecules and the matrix topography affected the diffusion and relaxation rates. In suspensions, both translational and rotational diffusion decreased with increasing casein concentrations due to increased restriction in the freedom of motion. Rotational diffusion was, however, less hindered than translational diffusion. After coagulation, translational diffusion increased but rotational diffusion decreased. Analysis of the  $T_2$  relaxation times obtained for probes of different sizes distinguished the free short-chain relaxation formed from a few monomeric units from (i) the relaxation of protons attached to long polymer chains and (ii) the short-chain relaxation attached to a rigid dendrimer core.

**KEYWORDS:** PEG, dendrimer, NPC, rennet gel, diffusion, relaxation

## I. INTRODUCTION

Caseins, a group of unique milk-specific, acid-insoluble phosphoproteins, represent around 80% of the total proteins in the milk of cattle and other commercial dairy species.<sup>1</sup> They are directly involved in the formation of dairy gels as they constitute the building blocks of the network. Most caseins in milk (94%) exist as large colloidal particles suspended in the aqueous phase. They are 50–600 nm in diameter (mean  $\approx$  150 nm) and called “casein micelles”,<sup>1</sup> which are very porous, highly hydrated and sponge-like colloidal particles containing about 3.2 g H<sub>2</sub>O/g protein.<sup>2</sup> Because of their commercial importance and extensive use in dairy products (such as cheese and yogurt), casein suspensions and gels have been extensively studied.

Molecular diffusion in dairy systems and in models of dairy systems has been studied by the use of techniques such as diffusion wave spectroscopy (DWS), multiple particle tracking (MPT), fluorescence recovery after photobleaching (FRAP), and pulsed field gradient NMR diffusometry. For example, DWS has been used to monitor the diffusion of casein particles during the acidification<sup>3,4</sup> and renneting<sup>5–9</sup> of undiluted skim milk. Multiple particle tracking has been used in an attempt to probe heterogeneity of acid milk gels and the microrheological properties of the protein network and aqueous phase voids, in the presence and absence of pectin, during and after gelation.<sup>10</sup> The sol–gel transition of a sodium caseinate solution undergoing gelation by acidification has also been studied by particle tracking. The Brownian diffusion of fluorescent microspheres with different surface coatings was used to probe spatial mechanical properties of the gels at the scale of micrometers.<sup>11</sup> Floury et al.<sup>12</sup> have recently used the fluorescence recovery after photobleaching (FRAP) technique to measure in situ and at the

microscopic scale the diffusion of FITC-dextran in a cheese model.

Several PFG-NMR self-diffusion studies have been performed on casein systems in which the self-diffusion coefficients of casein particles and polyethylene glycols (PEGs) of different molecular weights were measured at the micrometer scale for different casein concentrations. The diffusion behavior was related to the structure and dynamics of the casein matrix investigated. For example, Colsen et al.<sup>13</sup> and Le Feunteun et al.<sup>14–16</sup> studied the effects of casein concentration and PEG size on the diffusion coefficients of PEGs in native phosphocaseinate (NPC) suspensions and gels. PEG diffusion coefficients were found to be dependent on both casein concentration and PEG size. The effects of the gel structure on PEG diffusion were also studied by these authors. It was found that the diffusion rates of large polyethylene glycol (PEG) probes were enhanced after coagulation and that the rate of increase was dependent on the final gel microstructure. However, in all of the studies quoted above,<sup>13,14</sup> the diffusion of a molecule was measured at equilibrium, before and after perturbation of the system. In previous studies, Le Feunteun et al.<sup>15,16</sup> reported on the time change of the self-diffusivity of a small and a large PEG probes in a casein system during rennet-induced, acid-induced, and combined coagulation of a concentrated casein suspension, with the aim of investigating the structural changes taking place in the solution during coagulation. In another study,<sup>17</sup> Le Feunteun et al. monitored the

Received: November 20, 2012

Revised: April 15, 2013

Accepted: May 7, 2013

Published: May 7, 2013

diffusion of casein particles during the renneting of a concentrated casein micelle suspension (14% w/w). This study showed that the self-diffusion of both casein particles and soluble caseins can be determined simultaneously, and explained how their evolution can be related to key stages of the coagulation process. In a previous study,<sup>18</sup> we investigated the effects of casein structure on the diffusion behavior of PEG probes. The latter was studied in NPC and sodium caseinate (SC) suspensions where caseins are not structured into micelles but form self-assembled aggregates of 11 nm in radius. Two drastically different PEG diffusion behaviors were obtained in relation to differences in casein obstacle size (interparticle distance) and mobility between the two casein systems. The latter was studied in NPC and SC systems by measuring the casein self-diffusion coefficients in relation to casein concentration. Casein particles were found to behave as noninteracting hard spheres in a fluid, and their self-diffusion was inversely proportional to the solution viscosity measured macroscopically, up to a casein concentration that matched the onset of random close packing of the two casein systems (15 g/100 g H<sub>2</sub>O and 10 g/100 g H<sub>2</sub>O for NPC and SC systems, respectively). At higher concentrations, there was another regime (soft spheres) in which casein micelles and casein submicelles deformed, deswelled, and interpenetrated as the casein concentration increased.

Another important factor affecting the diffusion process is the shape of the diffusion molecules. For example, Wang et al.<sup>19</sup> have shown that star polymers, with a hydrophobic cholane core and four PEG arms, have a lower self-diffusion coefficient than linear PEGs at an equivalent hydrodynamic radius in PVA gels. This issue has not previously been explored in casein systems. In fact, the probes used to investigate casein systems have to date been polyethylene-glycol (PEG) polymers. The advantages of this type of polymer are the absence of interaction with proteins, excellent NMR sensitivity, and a low polydispersity index. However, these polymers are easily deformable and can change their shape according to their environment. They can therefore diffuse through small spaces as compared to their hydrodynamic diameter by adopting a more elongated conformation, which considerably complicates the interpretation of the diffusion results obtained in NPC suspensions. A preferred experimental design would therefore be to follow the diffusion of hard sphere probe particles through the matrix. Because it is difficult to obtain NMR signals from solid particles, flexible polymers with low molecular size polydispersity are used as probes instead. However, in more recent years, there has been greater interest in the use of dendrimer probes as diffusional probes.<sup>20–22</sup> Dendrimers, also known as starburst polymers, are spherical macromolecules and a class of regularly branched mono-dispersed polymers.<sup>23</sup> Dendrimer architecture consists of three domains: (1) the core, which can be a single atom or group of atoms, (2) branch units, which divide radially grown concentric layers termed generations, and (3) functional surface groups, which play a key role in determining the properties. Unlike classical polymers, dendrimers have a high degree of molecular uniformity, narrow molecular weight distribution, specific size and shape characteristics, and a highly functionalized terminal surface.<sup>23</sup> Dendrimer polymers are molecules of choice because of the good control of their molecular size and shape.

The purpose of the study presented here was to elucidate the effects of the shape and size of probes on their mobility in NPC suspensions and rennet casein gels. The translational and rotational diffusion of spherical dendrimer probes were therefore measured for the first time and compared to those of flexible PEG

probes in NPC suspensions and in a concentrated rennet casein gel (15 g/100 g H<sub>2</sub>O) using NMR diffusometry and NMR relaxometry. The advantage of coupling the two NMR methods was to probe the matrix at two different length scales. Moreover, both static and real-time NMR measurements were undertaken in this study and were performed at a casein gel concentration of 15 g/100 g H<sub>2</sub>O where casein micelles can be considered as hard spheres with no deformation of their shape.

## II. EXPERIMENTAL SECTION

**Materials.** Native phosphocaseinate powder was prepared in the INRA laboratory (Rennes). The detailed composition of this powder has already been described in ref 18. PEGs of different molecular weights  $M_w$  (615, 7920, 21 300, 32 530, and 93 000 g/mol) and low polydispersity indices ( $M_w/M_n = 1.07, 1.04, 1.06, 1.06, \text{ and } 1.06$ , respectively) were obtained from Varian Laboratories. Monodisperse polyamido-amine dendrimers with an ethylene diamine core, amido-amine branching units, and poly ethylene glycol (PEG) as surface group were purchased from Dendritic Nanotechnologies Inc. (U.S.). Five different generations (G2 (DNT-315), G3 (DNT-316), G4 (DNT-317), G5 (DNT-318), G6 (DNT-319)) were used. Sodium azide (Merck, Darmstadt, Germany) and sodium chloride (Sigma-Aldrich, Steinheim, Germany) with purity above 99% were used without purification. The chymosin solution used was Chymax-Plus purchased from Chr-Hansen (Arpajon, France).

**Preparation of Dispersions.** Rehydration of the powders with NaCl/water solution (0.1 M) was performed at room temperature over 36 h under constant stirring for casein concentrations below 15 g/100 g H<sub>2</sub>O, and at 40 °C over 24 h for casein concentrations above 15 g/100 g H<sub>2</sub>O. Sodium azide was added (0.02% w/w) to each solution to prevent bacterial development. The solutions were studied without adjustment of pH; the latter was ranging from 7.1 at 2.95 g/100 g H<sub>2</sub>O to 6.9 at 29.05 g/100 g H<sub>2</sub>O. Once the powder was totally rehydrated, 0.1% w/w of the probe was added to casein suspensions, regardless of the molecular weight. The molality was, thus, not constant and decreased with increasing probe size. The dry matter of all casein suspensions was controlled by measuring variations in weight after drying in an oven for 24 h at 103 °C. Casein concentrations were calculated from values of dry matter content in each casein suspension and the pure casein percentage of the dry matter.

**Enzymatic Coagulation.** All casein gels contained 15.31 g of casein to 100 g of H<sub>2</sub>O. For static diffusion measurements, casein gels were induced by addition of 4  $\mu$ L of chymosin in 10 g of NPC suspension. NMR tubes were placed in a water bath for 2 h at 30 °C, and measurements were carried out 24 h after inoculation. No gel shrinkage occurred within this interval. For real-time diffusion measurements, a chymosin dilution (1 mL in 99.0 g of distilled water) was added at time  $t = 0$  s to the casein suspension (70  $\mu$ L for 10 g of NPC suspension). The solution was then vigorously stirred for 3 min. Samples were then rapidly prepared for NMR and dynamic rheological measurements. No shrinkage of the gel was observed during the time scale of the experiments.

**Dynamic Light Scattering.** Dynamic light scattering measurements were performed on a Malvern Zetasizer Nano ZS instrument (Malvern Instruments, Worcestershire, UK). Size distribution of particles in solutions was obtained by measuring the light scattered by particles illuminated with a laser beam (scattering angle = 173°,  $T = 20$  °C) using the NNLS analysis method. The data measured were reported in log-normal intensity distribution.

**Rheology. Flow Measurements.** Flow measurements were performed with a contrives low-shear 30 viscometer (Ruislip, UK). The instrument was operated using a Couette geometry with inner and outer radii of 5.5 and 6 mm, respectively. All rheological experiments were performed at a fixed temperature of 20 °C. Measurements were repeated twice, showing very good reproducibility (within  $\pm 10\%$ ).

**Dynamic Rheological Measurements.** The viscoelastic properties of the enzymatic gels were studied with a AR2000 rheometer (Guyancourt, France) using a cone and plate geometry (Diameter 4 cm and angle 2°). Throughout the measurements, the temperature was maintained at 20

°C, and the sample was covered with a film of mineral oil to prevent evaporation. The storage modulus ( $G'$ ) and the loss modulus ( $G''$ ) were recorded at a frequency of 1 Hz, and the rheometer was programmed to adjust the stress automatically to provide a strain of 0.1%, which was found to be within the linear viscoelastic region of the sample.

**NMR Measurements.** All NMR measurements were performed on a 500 MHz spectrometer (Bruker Wissembourg, France) equipped with a dedicated field gradient probe (DIFF30 from Bruker, Wissembourg, France) with a static gradient strength of 1200 ( $\pm 0.2$ ) G/cm for an amplifier output of 40 A. NMR tubes (5 mm) were used, and all NMR measurements were performed at 20 °C.

A stimulated echo sequence using bipolar gradients (STE-BPP) and a 3–9–19 WATERGATE pulse scheme to suppress the water signal was used to measure self-diffusion coefficients. Diffusion coefficients were obtained using:

$$I(\delta, \Delta, g) = I_0 \exp \left[ -\gamma^2 g^2 \delta^2 \left( \Delta - \frac{\delta}{3} - \frac{\tau}{4} \right) D \right] \quad (1)$$

where  $I(\delta, \Delta, g)$  and  $I_0$  are the echo intensities in the presence of gradient pulses of strength  $g$  and the absence of gradient pulses, respectively,  $\gamma$  is the gyromagnetic ratio (for protons,  $\gamma = 26.7520 \times 10^7 \text{ rad T}^{-1} \text{ s}^{-1}$ ),  $g$  is the amplitude of the gradient pulse,  $\delta$  is gradient pulse duration,  $\Delta$  is the time between the leading edges of gradient pulses,  $\tau$  is the time between the end of each gradient and the next radiofrequency pulse, and  $D$  is the self-diffusion coefficient. Diffusion experiments were carried out with 32 different values of  $g$ , ranging from 20 to 900 G/cm, with  $\delta = 1$  ms. Sixteen scans were carried out, and the recycle delay was set at  $5 T_1$ . Depending on the molecular weight of the probe studied,  $\Delta$  was adjusted to obtain a diffusion distance  $z \approx 1.5 \mu\text{m}$  in the casein suspensions, in accordance with the Einstein equation  $z = (2\Delta D_{\text{Probe}})^{1/2}$ . This procedure enabled molecular probes to cover much greater distances than the casein micelle diameter.

All of the data processing was performed with Table Curve software (Ritme, Paris).

The Carr Purcell Meiboom Gill (CPMG) sequence, coupled with a presaturation pulse scheme for water proton signal suppression, was used to measure relaxation times ( $T_2$ ) of the ethoxylate methylene moieties at a chemical shift of 3.6 ppm. The relaxation decay curve for all probes was fitted accurately with a single exponential function:

$$I(2\tau) = I \exp \left[ -\left( \frac{2\tau}{T_2} \right) \right] \quad (2)$$

where  $I(2\tau)$  is the intensity of the NMR signal given at  $\tau$ ,  $I$  is the intensity at equilibrium for  $\tau = 0$ , and  $T_2$  is the spin–spin relaxation time.  $T_2$  measurements were undertaken with a  $\tau$ -value (time between 90° and 180° pulse) of 1 ms. Sixteen data points were acquired for each CPMG with 16 scan repetitions, and recycle delay was set at  $5 T_1$ .

The standard error in both probe self-diffusion coefficients and spin–spin relaxation times, estimated by the fitting procedure, was below 0.2%.

**Normalization of Diffusion Coefficients and Relaxation Times.** The effects of the soluble powder residues on probe self-diffusion were calculated according to the approach described in refs 14 and 15. All of the findings discussed in this Article are thus reduced self-diffusion coefficients defined as:  $D_r = D/D_0$ , where  $D$  is the probe self-diffusion coefficient measured in the suspension or the gel and  $D_0$  is the probe self-diffusion coefficient measured in the serum phase extracted from NPC suspensions. Similarly, the reduced  $T_2$  relaxation times calculated in suspensions were equal to the  $T_2$  values obtained in NPC suspensions divided by those obtained in the serum phase.

### III. RESULTS

**1. Dynamic Light Scattering.** The size distribution of a native phosphocaseinate solution (3 g/100 g water + 0.1 M NaCl) was determined from dynamic light scattering, presented as a single broad population distribution with casein particles from ~68 to ~459 nm in diameter (Figure 1). The average casein

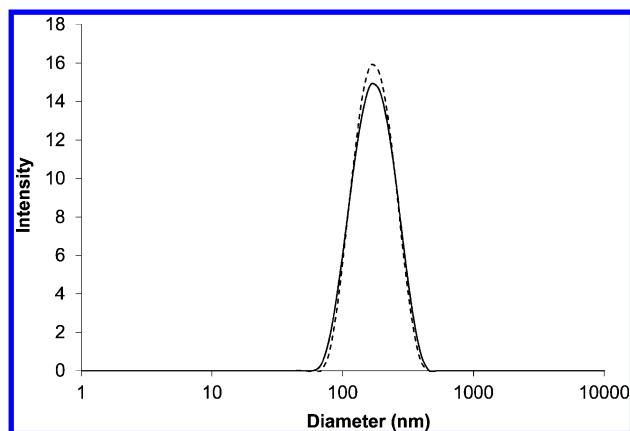


**Figure 1.** Log normal particle size distribution for a NPC solution (3 g/100 g H<sub>2</sub>O + 0.1 M NaCl) in the presence (—) and absence (---) of 0.1% w/w of G6 dendrimer at  $T = 20$  °C.

micelle diameter was 187 nm. These results were in very good agreement with values already reported by several authors.<sup>24–26</sup> As shown in Figure 1, the same casein size distribution was obtained in the presence of 0.1% w/w of G6 dendrimer.

**2. Rheology. a. Flow Measurements.** Figure 2 shows the shear rate dependence of the apparent viscosity for casein micelle

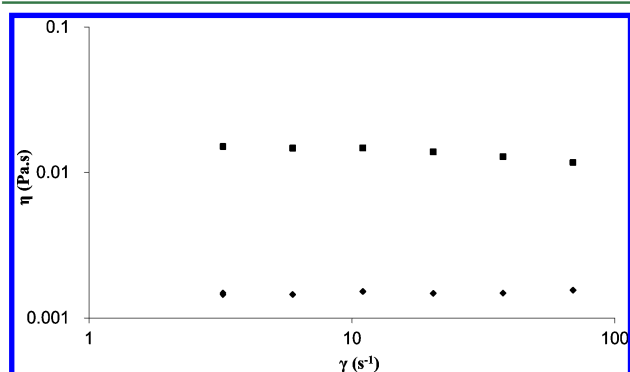


**Figure 2.** Shear rate dependence of apparent viscosity for NPC dispersions in H<sub>2</sub>O + 0.1 M NaCl, at  $T = 20$  °C, without adding any probes (PEG or dendrimer). Casein concentration from top to bottom: 15 and 3 g/100 g H<sub>2</sub>O.

(NPC) dispersions in H<sub>2</sub>O/NaCl with casein concentrations of 3 and 15 g/100 g H<sub>2</sub>O. The diluted NPC dispersion (3 g/100 g H<sub>2</sub>O) behaved as a Newtonian fluid over the range of shear rates investigated. At high casein concentrations, shear thinning occurred.

Viscosity values measured for the two NPC dispersions (3 and 15 g/100 g H<sub>2</sub>O) in the presence and absence of 615 g/mol PEG, and G2 and G6 dendrimers are given in Table 1. The viscosity values for the concentrated dispersion (15 g/100 g H<sub>2</sub>O) were measured at a shear rate of  $3 \text{ s}^{-1}$ . In agreement with previous studies,<sup>27</sup> the viscosity of NPC solutions increased from 1.52 to 15 mPa s with increasing casein concentration from 3 to 15 g/100 g water. The same viscosity values were obtained in the presence of 0.1% w/w of 615 g/mol PEG, G2 and G6 dendrimers, irrespective of casein concentration.

**b. Dynamic Storage Modulus and Phase Angle.** Figure 3 presents a typical plot of the storage modulus ( $G'$ ), the loss modulus ( $G''$ ), and the phase angle ( $\delta$ ) according to reaction time during the slow gel-forming process in the presence and absence of a G6 dendrimer.



**Table 1.** Viscosity of NPC Dispersions (3 and 15 g/100 g H<sub>2</sub>O + 0.1 M NaCl) in the Presence and Absence of 0.1% w/w of Probes (615, G2 and G6) Measured at  $T = 20\text{ }^{\circ}\text{C}$  and a Shear Rate of  $3\text{ s}^{-1}$

sample	viscosity (mPa s)/shear rate = $3\text{ s}^{-1}$
NPC (3 g/100 g H <sub>2</sub> O)	1.52
NPC (3 g/100 g H <sub>2</sub> O) + 615	1.51
NPC (3 g/100 g H <sub>2</sub> O) + G2	1.54
NPC (3 g/100 g H <sub>2</sub> O) + G6	1.53
NPC (15 g/100 g H <sub>2</sub> O)	15.1
NPC (15 g/100 g H <sub>2</sub> O) + 615	15.1
NPC (15 g/100 g H <sub>2</sub> O) + G2	14.9
NPC (15 g/100 g H <sub>2</sub> O) + G6	15

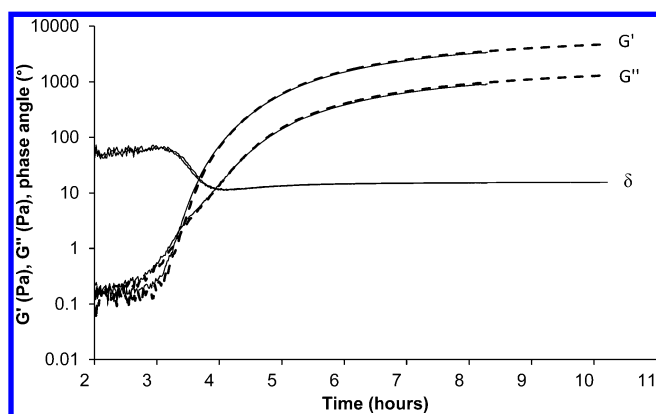


**Figure 3.** Evolution of storage modulus ( $G'$ ), loss modulus ( $G''$ ), and phase angle ( $\delta$ ) according to time after addition of chymosin to the casein suspension (15 g/100 g H<sub>2</sub>O + 0.1 M NaCl) in the presence (—) and absence (---) of 0.1% w/w of G6 dendrimer at  $T = 20\text{ }^{\circ}\text{C}$  and  $\text{pH} \approx 7$ .

The time at which  $G'$  and  $G''$  are equal is often used to define the “gel time” parameter. In this study, it was found to be  $t_{\text{gel}} = 3\text{ h } 20\text{ min}$  in the presence and absence of a G6 dendrimer. This indicates that the addition of low concentrations (0.1% w/w) of dendrimer has no effect on the formation of the casein network.  $G'$  and  $G''$  continued to increase after the sol–gel transition. This indicated an increase in the gel stiffness through reorganization of the gel structure.

**3. Diffusion and Relaxation by NMR. a. Self-Diffusion and Relaxation of Probe in Water.**  $^1\text{H}$  NMR  $T_2$  relaxation times and the self-diffusion coefficients of dendrimers and PEGs in water/0.1 M NaCl are presented in Table 2. The  $^1\text{H}$  NMR  $T_2$  relaxation times pertain to the ethoxylate methylene moieties at a chemical shift of 3.6 ppm. The hydrodynamic radius of the probes was calculated from the  $D$  values using the Stokes–Einstein equation:

$$R_h = \frac{k_B T}{6\pi\eta D} \quad (3)$$

where  $T$  is the temperature in kelvin,  $k_B$  is the Boltzmann constant ( $1.38 \times 10^{-23}\text{ J K}^{-1}$ ), and  $\eta$  is the viscosity of the aqueous phase ( $1 \times 10^{-3}\text{ Pa s}$  at  $20\text{ }^{\circ}\text{C}$ ).

On the basis of these results, PEG–dendrimer trios and couples with similar hydrodynamic radii could be recognized: (i) 7920/G2;G3, (ii) 21300/G5, and (iii) 32530/G6. In the following, PEG and dendrimers are referred to as  $G_X$  and  $\text{PEG}_X$ , with  $X$  being equal to the hydrodynamic radius of these diffusional probes.

**Table 2.**  $^1\text{H}$  NMR  $T_2$  Relaxation Times, Self-Diffusion Coefficients, and the Corresponding Hydrodynamic Radii of Different Dendrimer Generations (A) and PEG Molecular Weights (B)<sup>a</sup>

A			
	$D\text{ (m}^2\text{ s}^{-1}\text{)}$	$R_h\text{ (nm)}$	$T_2\text{ (s)}$
G2	$7.54 \times 10^{-11}$	2.84	0.485
G3	$6.10 \times 10^{-11}$	3.51	0.450
G4	$4.87 \times 10^{-11}$	4.40	
G5	$4.16 \times 10^{-11}$	5.16	0.385
G6	$3.42 \times 10^{-11}$	6.27	0.338
B			
PEGs	$D\text{ (m}^2\text{ s}^{-1}\text{)}$	$R_h\text{ (nm)}$	$T_2\text{ (s)}$
615	$2.7 \times 10^{-10}$	0.79	0.620
7920	$6.77 \times 10^{-11}$	3.16	0.528
21 300	$3.99 \times 10^{-11}$	5.37	0.524
32 530	$3.06 \times 10^{-11}$	7	0.522
93 000	$1.62 \times 10^{-11}$	13.22	0.518

<sup>a</sup>Data obtained from NMR measurements of 0.1% w/w of probes in a H<sub>2</sub>O/NaCl solution (0.1 M) at  $20\text{ }^{\circ}\text{C}$ .

As seen in Table 2,  $T_2$  relaxation times decreased from 0.485 to 0.338 s with increasing dendrimer molecular weights ( $M_w$ ) from 12 628 (G2) to 207 988 (G6) g/mol.  $T_2$  relaxation times for PEGs were longer and decreased from 0.620 to 0.528 s with increasing PEG molecular weights from 615 to 7920 g/mol. However, when  $M_w$  exceeded 7920 g/mol,  $T_2$  values exhibited minor variations, in the order of 12 ms or less.

**b. PEG and Dendrimers Reduced Self-Diffusion in NPC Suspensions and Gels.** The self-diffusion coefficients of a PEG/dendrimer trio and a PEG/dendrimer couple having similar hydrodynamic radii ((i)  $\text{PEG}_{3.16}$  vs  $G_{2.84}$  and  $G_{3.51}$ , (ii)  $\text{PEG}_7$  vs  $G_{6.27}$ ) were measured at  $20\text{ }^{\circ}\text{C}$  in NPC suspensions, with casein concentrations ranging from 3 to 29 g/100 g of water, and in a concentrated casein gel with a casein concentration of 15 g/100 g H<sub>2</sub>O (Figure 4). The absence of restricted diffusion (in suspensions and gels), at the length-scale studied ( $\sim 1.5\text{ }\mu\text{m}$ ), was verified for PEGs and dendrimers by varying the diffusion delay corresponding to a diffusion distance of between 0.3 and  $2.4\text{ }\mu\text{m}$  in suspensions and 0.58 and  $4.07\text{ }\mu\text{m}$  in gels. No variation in the diffusion coefficient measured occurred (data not shown).

Probe self-diffusion coefficients were found to be dependent on both casein concentration and their own size; the probe diffusion decreased with increasing casein concentrations, and the probe self-diffusion reduced with size for a given concentration. This effect was observed for PEG as well as for dendrimer probes. The reduction in diffusion coefficients was greater for larger probes, giving  $D_r \approx 0.61$  and 0.49 for  $\text{PEG}_{3.16}$ / $G_{2.84}$ / $G_{3.51}$  and  $\text{PEG}_7$ / $G_{6.27}$ , respectively, at a casein concentration of 15 g/100 g H<sub>2</sub>O. However, at higher casein concentrations, the diffusion coefficient was smaller for dendrimers as compared to PEGs despite the fact that the probes were of similar size. For example, at a casein concentration of 29 g/100 g H<sub>2</sub>O, the  $D_r$  of a 6.27 nm sized dendrimer and a 7 nm sized PEG ( $G_{6.27}$  dendrimer and  $\text{PEG}_7$ ) were 0.14 and 0.22, respectively. This highlights the effects of probe shape and flexibility on self-diffusion behavior.

After coagulation, the self-diffusion of PEG and dendrimer couples with similar  $R_h$  increased in the same manner. For the small probes ( $R_h \approx 3\text{ nm}$ ), the increase was not very significant, and hence the rennet coagulation had no influence on the

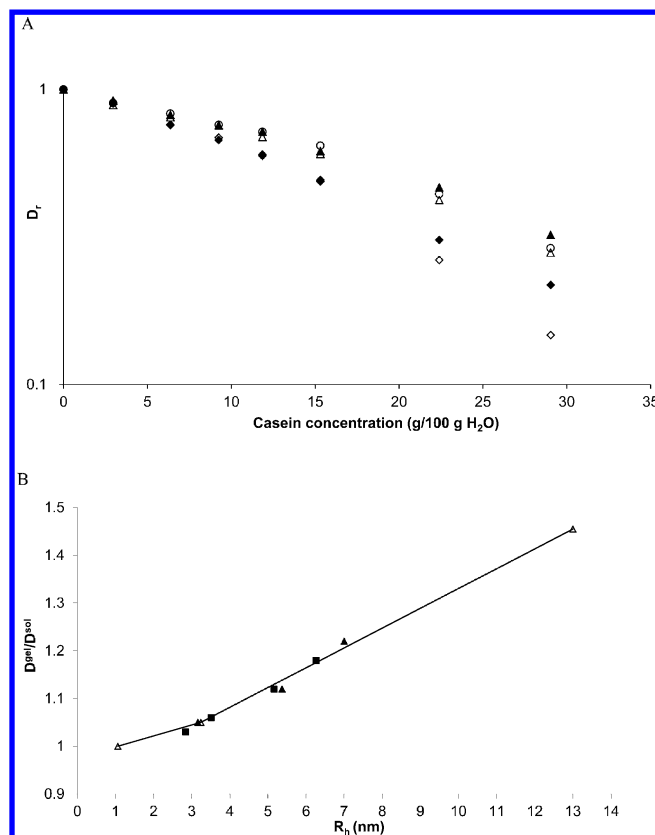


**Figure 4.** (A) Comparison of reduced self-diffusion coefficients of 0.1% w/w of PEG<sub>3.16</sub> (▲)/PEG<sub>7</sub> (◆) and G<sub>2.84</sub> (○); G<sub>3.51</sub> (△)/G<sub>6.27</sub> (◇) dendrimers in relation to casein concentrations in NPC suspensions measured at  $T = 20^\circ\text{C}$ . (B)  $D^{\text{gel}}/D^{\text{sol}}$  ratios obtained for PEGs (▲) and dendrimers (■) of various sizes in a concentrated rennet gel (15 g/100 g H<sub>2</sub>O + 0.1 M NaCl) measured at  $T = 20^\circ\text{C}$ . Empty triangles (△) correspond to previously reported data<sup>14,15</sup> obtained in rennet casein gels prepared at the same casein concentration and temperature.

diffusion of small probes. However, for the four largest probes ( $R_h \approx 5\text{--}7\text{ nm}$ ), the effects of coagulation were greater as the size of the probe became larger. All of these findings were in very good agreement with those already reported by Le Feunteun et al.,<sup>14</sup> who studied the effects of coagulation on the diffusion of PEG probes with hydrodynamic radii of 0.8, 3.24, and 13.3 nm (Figure 4B).

**c. PEG and Dendrimer  $^1\text{H}$  NMR  $T_2$  Relaxation Times in NPC Suspensions and Gels.** In parallel to self-diffusion measurements,  $^1\text{H}$  NMR  $T_2$  relaxation times were measured for each of the probes in casein suspensions with casein concentrations ranging from 3 to 22 g/100 g of water. Figures 5 and 6 illustrate the dependence of the relaxation times on casein concentration and the molecular size of the probe. Figures 5A and 6A show that (i) probe  $^1\text{H}$  NMR  $T_2$  relaxation times decreased with increasing casein concentrations: the values obtained varied between 0.62 and 0.21 s for PEGs and between 0.48 and 0.18 s for dendrimers, depending on the casein concentration and the molecular size of the probe; and (ii) PEGs and dendrimers did not show a similar decreasing relaxation trend. In the case of dendrimers,  $T_2$  relaxation followed a similar decreasing trend whatever the generation. All data collapsed onto a master curve when the reduced relaxation time was plotted as a function of casein concentration (Figure 6A). In the case of PEG probes, however, different decreasing curves were obtained depending on the molecular weight of the probe. It can clearly be seen in Figures 5B

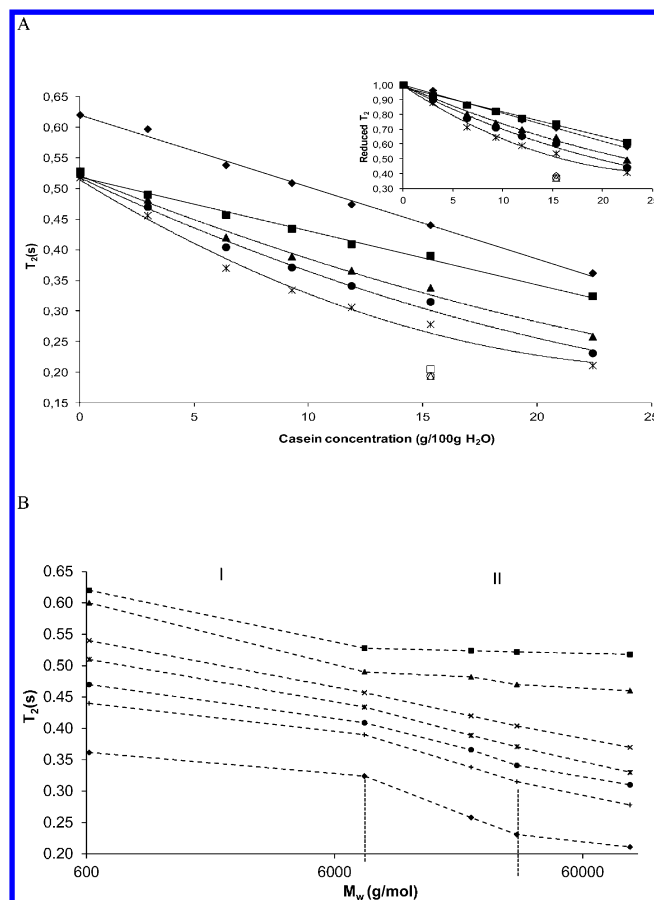


**Figure 5.** (A) Relaxation time  $T_2$  of 0.1% w/w of PEGs as a function of casein concentrations in NPC suspensions measured at  $T = 20^\circ\text{C}$ . PEG probes from top to bottom: 615, 7920, 21 300, 32 530, and 93 000 g/mol. Reduced  $T_2$  relaxation times are shown in the inset panel. Solid lines are guides for the eyes. Empty shapes correspond to the relaxation time  $T_2$  obtained for the 7920 (□), 21 300 (△), and 32 530 (○) g/mol PEGs in the concentrated casein gel (15 g/100g H<sub>2</sub>O + 0.1 M NaCl) measured at  $T = 20^\circ\text{C}$ . (B) Molecular weight dependence of the PEGs transverse relaxation time for various casein concentrations (from top to bottom): 0, 2.88, 6.43, 9.22, 11.86, 15.35, and 22.4 g/100 g H<sub>2</sub>O.

and 6B that two domains of chain dynamics could be determined for PEGs, while linear variations occurred for dendrimers. The crossover between the two domains labeled I and II occurred when the PEG molecular weight was about 7920 g/mol. Within the first domain, as for dendrimers, the PEG relaxation rates measured in NPC suspensions for different casein concentrations were similarly dependent on molecular weight. In contrast, the relaxation rates behaved very differently in domain II (below 7920 g/mol). At zero casein concentration and in the diluted casein system (2.95 g/100 g H<sub>2</sub>O),  $T_2$  was almost independent of the PEG chain length, but became dependent when casein concentrations increased. A clear double break behavior was also visible for the casein concentrations greater than 12 g/100 g H<sub>2</sub>O. Intersection of the straight line was observed at  $M_w = 32\,530\text{ g/mol}$ .

On the other hand,  $^1\text{H}$  NMR  $T_2$  relaxation times surprisingly decreased after coagulation (Figures 5A and 6A), reflecting reduced rotational probe mobility in casein gels. The dependence of the relaxation times on the molecular weights of dendrimers and PEGs in the concentrated casein suspension and the rennet gel is illustrated in Figure 7. For dendrimer probes,  $T_2$  relaxation times varied with increasing dendrimer molecular

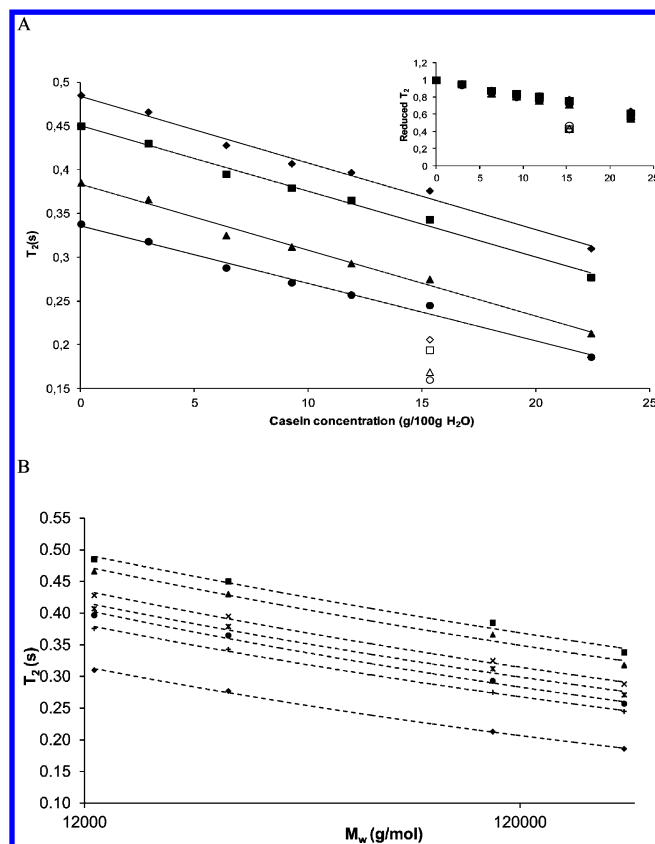


**Figure 6.** (A) Relaxation time  $T_2$  of 0.1% w/w of dendrimers as a function of casein concentrations in NPC suspensions measured at  $T = 20^\circ\text{C}$ . Dendrimers from top to bottom: G2, G3, G5, and G6. Reduced  $T_2$  relaxation times are shown in the inset panel. Solid lines are guides for the eyes. Empty shapes correspond to the relaxation time  $T_2$  obtained for the G2 ( $\diamond$ ), G3 ( $\square$ ), and G5 ( $\triangle$ ) and G6 ( $\circ$ ) dendrimers in the concentrated casein gel (15 g/100 g  $\text{H}_2\text{O}$  + 0.1 M NaCl) measured at  $T = 20^\circ\text{C}$ . (B) Molecular weight dependence of the dendrimers transverse relaxation time for various casein concentrations (from top to bottom): 0, 2.88, 6.43, 9.22, 11.86, 15.35, and 22.4 g/100 g  $\text{H}_2\text{O}$ .

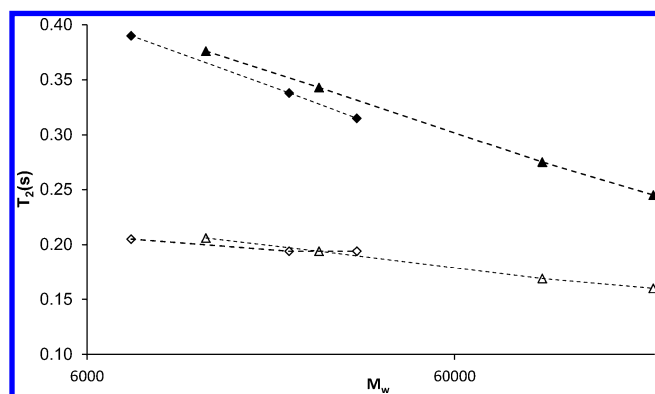


**Figure 7.** Molecular weight dependence of PEG (diamond) and dendrimer (triangle) transverse relaxation times in the concentrated casein suspension (solid shapes) and the gel (open shapes) with a casein concentration of 15 g/100 g  $\text{H}_2\text{O}$ .

weight from 0.376 to 0.245 s in the casein suspension and from 0.206 to 0.160 s in the gel. For PEG probes,  $T_2$  relaxation times varied from 0.390 to 0.315 s in the casein suspension with increasing PEG molecular weight from 7920 to 32530. However,

in the rennet gel,  $T_2$  hardly varied (less than 10 ms) when the PEG molecular weight increased from 7920 to 32530 g/mol.

To obtain greater understanding of the impact of structural changes in the casein matrix on probe mobility during coagulation, we monitored the self-diffusion coefficients and the relaxation rates of the G6 dendrimer during renneting of the concentrated casein micelle suspension. This revealed how and when probe diffusion and relaxation times varied during the coagulation induced by chymosin action. As shown in Figure 8, relaxation of the G6 dendrimer remained stable during the first stage of coagulation, that is, the enzymatic phase. Immediately after the aggregation of the resulting para-casein micelles (gel formation), relaxation decreased rapidly and continued to decrease gradually throughout the experiment until it stabilized after approximately 20 h. However, diffusion of the G6 dendrimer was unaffected by the first two stages of coagulation, that is, the enzymatic and the aggregation phases, and started to change after approximately 5 h of coagulation, approximately 2 h after gel formation. Diffusion results were in agreement with those already obtained by Le Feunteun et al.,<sup>15</sup> who monitored the diffusion of a 96750 g/mol PEG ( $R_h = 13.3$  nm) in a concentrated rennet gel.

#### IV. DISCUSSION

Previous studies<sup>13,14</sup> have improved our understanding of the mechanisms of self-diffusion of linear and deformable PEG probes of various sizes in NPC suspensions and gels. It has been shown that PEG diffusion in casein suspensions is greatly dependent on both the volume fraction occupied by casein particles and the probe size. The reduction in the self-diffusion coefficient for a given volume fraction of casein particles is smaller for smaller probes. This phenomenon was first explained by assuming a model with two diffusion pathways, one around the casein particles and one through these particles. Such a model was proposed because casein particles are known to be porous and highly hydrated.<sup>28</sup> On the other hand, because PEGs are flexible and easily deformable, they can diffuse through small spaces as compared to their hydrodynamic diameter by adopting a more elongated conformation, as described by the reptation model of De Gennes and proved by other studies.<sup>19,29</sup> However, the results of our previous study<sup>18</sup> dealing with the effects of the casein system (NPC ( $R_{h \text{ casein}} = 100$  nm) and SC ( $R_{h \text{ casein}} = 11$  nm) systems) on PEG diffusion indicated that the extra-particle mechanism, which is the only one to be considered in the case of SC suspensions, was sufficient to explain the differences observed in the values of the diffusion coefficients according to probe size. The results assumed that intracellular diffusion mechanism adopted in the NPC system would be negligible, and results could be explained by taking into account the size of the probe and the density of the system. This explanation was proposed because PEG diffusion was much more attenuated in SC than in the NPC system. If intracellular diffusion exists, we would have observed the opposite situation, as PEG would be more constrained inside the micelle and hence would experience fewer obstruction effects when diffusing around casein aggregates in SC dispersions.

To further validate our hypotheses and to achieve a better understanding of probe diffusion in NPC suspensions and gels, a preferred experimental design is proposed below to follow the diffusion of hard spherical probe particles such as dendrimers with fixed dimensions through the casein matrix. Because of their spherical shape, dendrimers cannot diffuse inside the micelle. Only extracellular diffusion is possible for this kind of probe. The

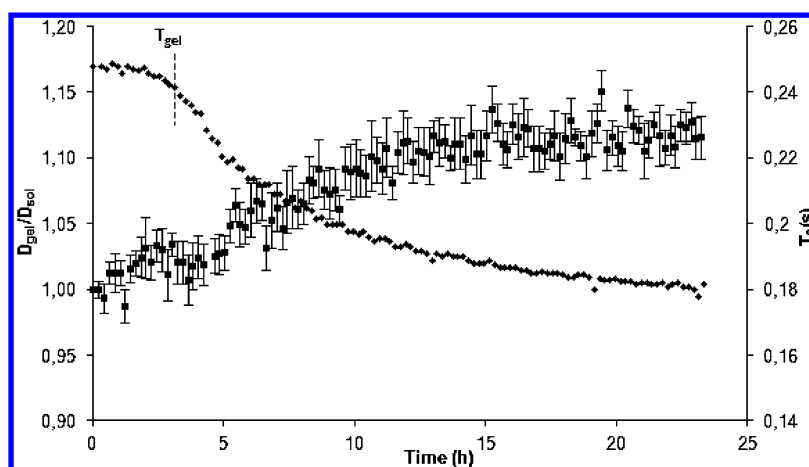


**Figure 8.** Evolution of the G6 dendrimer (0.1% w/w) self-diffusion coefficients (■) and  $T_2$  relaxation times (◆) over time after addition of chymosin to the concentrated casein suspension (15 g/100 g  $H_2O$  + 0.1 M NaCl) at  $T = 20\text{ }^{\circ}\text{C}$  and  $\text{pH} \approx 7$ .

results obtained for the combined study of diffusion and relaxation are discussed below.

**Mobility of PEG and Dendrimer Probes in NPC Suspensions.** *i. Self-Diffusion.* The onset of close-packing, where casein micelles come into direct contact, occurs in NPC suspensions at a casein concentration of about 15 g/100 g water.<sup>18,30</sup> Below the close packing limit, PEG and dendrimer couples (with similar  $R_h$ ) have similar diffusion behaviors (Figure 9 in the Supporting Information). This finding is consistent with our previous results,<sup>18</sup> which indicated that at a low obstacle density (between 2.88 and 15 g/100 g  $H_2O$ ) the obstruction mechanism induced by casein micelles has no constraints on the conformation of PEGs, which remain in a spherical random coil form. If intramolecular diffusion exists, self-diffusion of PEG should be slower than for dendrimer as it should experience more obstruction effects when diffusing inside the micelle. In the light of our results, and in agreement with our previous study,<sup>18</sup> intramolecular diffusion as earlier proposed for NPC systems can no longer be taken into consideration. Only an extra-micellar diffusion mechanism can exist regardless of the probe size and deformability. Above close-packing probes continued to diffuse, and differences occurred in their diffusion behavior; PEGs diffused faster than dendrimers, and the differences in self-diffusion became greater as the size of the probe increased. Probe diameter approached the pore size of the casein matrix with increasing casein concentrations (beyond 15 g/100 g  $H_2O$ ) and probe size.<sup>18</sup> The probes therefore diffused less freely through a dense array of obstacles, which hindered their mobility in a size-dependent manner. Hindrance to PEG diffusion was less because it is capable of changing its shape to move through the concentrated casein solution by adopting an ellipsoidal random coil form,<sup>18</sup> while a dendrimer sphere has no flexibility and thus encounters greater resistance.

*ii.  $^1\text{H}$   $T_2$  Relaxation Times.* While the self-diffusion coefficient reflects displacement of the molecule within the casein matrix over micrometer distances, the  $T_2$  relaxation time reflects the rotational or local mobility of molecules at the nanometer scale.  $^1\text{H}$   $T_2$  relaxation can be linked to any molecular motion that can induce fluctuating local magnetic fields. There are several distinct mechanisms occurring at the molecular level that can contribute to relaxation, but the most common mechanism is the magnetic dipole–dipole interaction, which is assumed to be responsible for the relaxation of transverse magnetization in this study.

The chain length of the PEG probes used in this study increased significantly (from 615 to 93 000 g/mol PEG). The results obtained at zero casein concentration (Figures 5 and 6) reflect greater mobility for the low molecular weight PEG probes, consistent with the increasing contribution of the overall tumbling of the molecule to the relaxation. The striking result of these experiments was the relatively low molecular weight of PEGs, corresponding to a critical size of 180 monomer units, above which the  $T_2$  relaxation became almost size-independent. This result demonstrates the local nature of the motions responsible for the  $T_2$  relaxation in polymer chains in an  $H_2O$  solution. Above this critical size, the overall tumbling was much slower than the local motions, and, therefore, its contribution to the relaxation was negligible. Therefore, for PEG polymers in  $H_2O$ , the contribution of segmental motion to  $^1\text{H}$   $T_2$  is the dominant factor rather than that of the rotational motion of a whole molecule. In contrast to PEG polymers, the dendrimer macromolecules were characterized by PEG terminal function groups located on the exterior, with a uniform chain length of 587 g/mol. Only the number of chains doubled from one generation to the next. The length of this chain was therefore short, and the size was close to that of the 615 g/mol PEG. As the length of this short chain does not vary, the local mobility of PEG chains was the same and only affected by the overall dendrimer tumbling, which depended on the overall dendrimer size. The effect of dendrimer core rigidity manifested itself through the values of  $T_2$ , which were found to be much lower than those of the 615 g/mol PEG. The  $T_2$  relaxation times measured thus reflected the global mobility of the dendrimer molecules.

Probe relaxation times decreased significantly in the presence of casein micelles. In many studies performed by other authors, reduction of  $T_2$  relaxation times has been attributed to an intermolecular interaction between a probe and the network,<sup>31,32</sup> or to changes in viscosity.<sup>33</sup> Attention has also focused on the effects of polymer chain length on  $T_2$  relaxation time in entangled polymer systems and prior to reptation motion.<sup>34–37</sup> To our knowledge, no studies exist concerning the effects of PEG/PEO polymer chain length on  $T_2$  relaxation times measured in dilute and semidilute protein systems.

In cases of interaction, there are two types of exchange processes between free PEG probes and those interacting with the casein matrix. Intercompartmental exchange can be characterized as slow and fast. Under slow exchange, the relaxation will be biexponential; that is, relative components of



the signal will correspond closely to the volume fractions of the physical compartments. Under fast exchange, the relaxation will be monoexponential, the single relaxation rate being the weighted volume-average of the two relaxation rates and being dependent on the pulse spacing used. However, our results showed that (i) the addition of 0.1% w/w of probes had no effect on the size of the casein particles, on the viscosity values of the suspensions, or on the casein network formation, (ii) in our  $^1\text{H}$   $T_2$  experiments, PEGs and dendrimers in casein suspensions had a single component for the relaxation behavior, and (iii) there was no dependence of the transverse relaxation rate of PEG on the pulse spacing for a casein concentration of 15 g/100 g water. The experimental  $T_2$  values remained stable when varying the echo time between 50  $\mu\text{s}$  and 2 ms (data not shown). All of these results confirm the absence of interaction between casein particles and probes and exclude the interpretation based on slow and fast exchange of molecules. Therefore, only dipole–dipole interaction was to be considered to explain the changes in  $T_2$  values.

Taking into account the Stokes–Einstein–Debye equation, it is possible to connect the  $T_2$  variations with changes in the solvent viscosity. However, microviscosity is not easily quantified, and there is no indication of its variation in casein suspensions according to casein concentration. On the other hand, dipole–dipole interactions are known to have a considerable impact on changes in  $T_2$  values. These dipolar effects can be influenced both by intermolecular interactions and by changes in the overall environment. The variation in relaxation times for a given polymer with increasing casein concentration can be attributed to increased restriction of its freedom of motion with increasing casein concentrations. Comparison of the reduced dendrimer self-diffusion (Figure 4A) and its  $T_2$  relaxation times (Figure 6A) revealed that the retardation of the probe rotation was substantially less than the retardation of its translation (diffusion) in concentrated casein suspensions. This indicates that dendrimer mobility was less restricted over small distances than over large ones. This was also true for the PEG probes. In contrast to the reduced diffusion results for dendrimers, which were affected by the casein concentration and probe size, reduced dendrimer  $T_2$  relaxation times depended similarly on the casein concentration whatever the probe size. This was not the case for PEG polymer chains because their flexibility led to variations in the contribution to the relaxation of the local segmental motion and the global or long-range motions of large chains. In diluted casein systems ( $C < 6.43$  g/100 g  $\text{H}_2\text{O}$ ), the PEG  $T_2$  relaxation was governed by the local mobility of the chain as in water solutions. When the casein concentration increased, the local mobility was restricted, and the overall tumbling of the probe played a major role in the relaxation times even for a relatively large chain size. This result explains the dependence of  $T_2$  relaxation times on probe molecular weights in domain II for casein concentrations  $\geq 6.43$  g/100 g  $\text{H}_2\text{O}$ . At higher concentrations ( $>12$  g/100 g  $\text{H}_2\text{O}$ ), the mobility of the 93 000 g/mol PEG was found to be greater than expected.  $T_2$  relaxation times measured for this probe in such concentrated systems reflect either higher mobility, due to its ability to undergo conformational changes,<sup>18</sup> or further anisotropy in the motion of probes, which can be attributed to the increase in obstruction effects induced by casein proteins. The anisotropic motion of the probe chains on the NMR time scale may cause residual dipolar coupling, which affects the values of the  $T_2$  measured.

#### Mobility of PEG and Dendrimer Probes in a Concentrated Casein Rennet Gel. i. Self-Diffusion.

The coagulation induced by chymosin action is generally broken into three phases: enzyme action, aggregation, and gel aging.<sup>38–41</sup> First, the enzyme specifically splits off the  $\kappa$ -casein located at the surface of the supramolecular edifice. This reduces the steric and electrostatic repulsion between casein particles, and the suspension becomes unstable. In the second phase, the resulting *para*-casein micelles spontaneously aggregate and form a microscopic network. In this study, this phenomenon was characterized by the rapid increase in  $G'$  and  $G''$  and the sudden decrease in  $\delta$  between 3 and 4 h (Figure 3). The transition from solution to gel occurred at  $t = 3$  h 20 min for slow coagulation, induced by addition of 4  $\mu\text{L}$  of chymosin in 10 g of NPC suspension at 20  $^\circ\text{C}$ , and within a few minutes for the fast coagulation induced by addition of 70  $\mu\text{L}$  of a chymosin dilution (1 mL in 99.0 g of distilled water) in 10 g of NPC suspension at 30  $^\circ\text{C}$  (data not shown). Finally, the third phase corresponds to the aging of the gel and is characterized by the occurrence of structural changes in the casein network, which give rise to local matrix fusion and compaction, resulting in a gel with larger pores and greater permeability.<sup>39,42–45</sup> Although the stages are different in nature, they are not clearly separated in time. The aggregation phase always starts before the end of the enzymatic reaction<sup>6,17,40,41,46</sup> and occurs at an even lower degree of  $\kappa$ -casein hydrolysis when the casein concentration is increased.<sup>17,39,47</sup> This is believed to be caused by a smaller mean free distance between casein micelles, which increases the collision frequency, and higher concentrations of ionic calcium, which reduce the electrostatic repulsion in concentrated dairy solutions.<sup>39,47</sup> On the basis of the reported results,<sup>17,39,47</sup> the percentage of proteolysis at gel formation for a casein concentration of 15 g/100 g  $\text{H}_2\text{O}$  is 40%. The enzymatic reaction continues to occur long past the gelation point.

As was already reported by Le Feunteun et al.<sup>14–16</sup> and Colson et al.,<sup>13</sup> the significant increase in the self-diffusion of large probes after coagulation can thus be explained on the basis of the network rearrangements that lead to particle fusion and compaction and consequently to a dramatic decrease in the casein particle size and an increase in protein–protein interactions.<sup>48</sup> All of these changes result in a structure where molecules have more free space to diffuse.

The effects of the gel structure on the solute diffusion have also previously been studied using NMR diffusometry by several authors in different matrixes.<sup>20,49–51</sup> Strong connection has been found between the gel structure and the probe diffusion in both  $\kappa$ -Carrageenan<sup>20,50</sup> and whey protein<sup>51</sup> gels. The diffusion behavior has been determined mainly by the void size, which in turn has been defined by the state of aggregation of the matrix. The effects of coagulation have also been investigated using simulation methods,<sup>52</sup> which have shown that the diffusion of a spherical probe in hard sphere suspensions and gels is mainly dependent on the volume fraction that is accessible to the diffusing particle.

However, the striking result of these experiments was that spherical dendrimer probes and flexible PEG probes of similar sizes showed the same increase in diffusion behavior after coagulation despite the differences in their structure. If small PEG probes could enter casein aggregates, their diffusion would be slower than that of dendrimers because they would experience more obstruction effects when diffusing inside the aggregates. In addition, during the rearrangement process, the fused particles may be accompanied by a reduction in strand porosity through



shrinkage. Under the hypothesis that PEGs diffuse through the strands, these effects would lead to an increase in the obstruction effect for PEG molecules and thus a decrease in the diffusion coefficient after coagulation. In the light of our results showing an increase instead of a decrease in the probe self-diffusion coefficient, the intra-aggregate diffusion pathway already proposed in NPC rennet gels is no longer valid. Only an extra-aggregate diffusion mechanism can exist, regardless of the probe size and deformability, as in the case of NPC suspensions. The absence of significant effect of coagulation for the smallest PEGs with  $R_h \leq 3$  nm may be attributed to lower sensitivity to a change in voluminosity (as observed in suspensions) because of their small size.

**ii.  $^1\text{H}$   $T_2$  Relaxation Times.** The local mobility of the matrix is an important issue that has to be taken into consideration. Indeed, several NMR studies have demonstrated that casein micelle, despite its large size, contains a highly mobile protein segment, which explains the narrow peak in the NMR spectra.<sup>53</sup> Thus, the mobility of the probe molecule will most probably be affected by the motion of these segments. The coagulation of our concentrated casein sample may be visualized by the formation of a network backbone during the sol–gel transition, which was progressively reinforced upon further incorporation of particles during the aging phase accompanied by the loss of the highly mobile  $\kappa$ -casein macro-peptide.<sup>53</sup> This slow casein particle aggregation process was responsible for delayed development of maximum firmness in the gel (Figure 3). As the gel became denser, the local motion of casein particles became slower as a result of the formation of small clusters or network-like structures. This reduced motion can explain the decrease in  $T_2$  relaxation times of probes in gels and the slope variation between suspensions and gels of the line showing the dependence of dendrimer and PEG  $T_2$  relaxation times on molecular weight (Figure 7).

On the other hand, a decrease in casein mobility might be thought to result in a decrease in probe self-diffusion, but this reasoning would overlook the fact that the structural changes lead to a more open network gel structure.

## ■ ASSOCIATED CONTENT

### Supporting Information

Two figures: Figure 9, which shows the variation in  $D_R^{\text{PEG}}/D_R^{\text{dend}}$  values as a function of casein concentration in NPC suspensions, and another figure, which presents a  $^1\text{H}$ -PFG-NMR spectrum of the casein suspension we studied. This material is available free of charge via the Internet at <http://pubs.acs.org>.

## ■ AUTHOR INFORMATION

### Corresponding Author

\*Tel.: 33 (0)223482121. Fax: 33(0)223482115. E-mail: francois.mariette@irstea.fr.

### Funding

We thank the Regional Council of Brittany and Unilever (Netherlands) for financial support.

### Notes

The authors declare no competing financial interest.

## ■ ACKNOWLEDGMENTS

We are grateful to Arnaud Bondon for access to the NMR facilities of the PRISM Research Platform (Rennes, France). We also thank Marie-Helene Famelart and Florence Rousseau (INRA Rennes, UMR STLO) for their assistance with the

rheological and dynamic light scattering experiments. IRM-Food team has been awarded ISO 9001 certification for its activities related to research.

## ■ REFERENCES

- (1) Holt, C. Structure and stability of bovine casein micelles. *Adv. Protein Chem.* **1992**, *43*, 63–151.
- (2) de Kruif, C. G.; Huppertz, T. Casein micelles: Size distribution in milks from individual cows. *J. Agric. Food Chem.* **2012**, *60*, 4649–4655.
- (3) Cucheval, A.; Vincent, R.; Hemar, Y.; Otter, D.; Williams, M.; Vincent, R. R.; Williams, M. A. K. Diffusing wave spectroscopy investigations of acid milk gels containing pectin. *Colloid Polym. Sci.* **2009**, *287*, 695–704.
- (4) Alexander, M.; Piska, I.; Dalgleish, D. G. Investigation of particle dynamics in gels involving casein micelles: A diffusing wave spectroscopy and rheology approach. *Food Hydrocolloids* **2008**, *22*, 1124–1134.
- (5) Alexander, M.; Dalgleish, D. G. Application of transmission diffusing wave spectroscopy to the study of gelation of milk by acidification and rennet. *Colloids Surf., B* **2004**, *38*, 83–90.
- (6) Sandra, S.; Alexander, M.; Dalgleish, D. G. The rennet coagulation mechanism of skim milk as observed by transmission diffusing wave spectroscopy. *J. Colloid Interface Sci.* **2007**, *308*, 364–373.
- (7) Horne, D. S. Studies of gelation of acidified and renneted milks using diffusing wave spectroscopy. *Milchwissenschaft* **1991**, *46*, 417–420.
- (8) Gaygadzhiev, Z.; Alexander, M.; Corredig, M. Sodium caseinate-stabilized fat globules inhibition of the rennet-induced gelation of casein micelles studied by Diffusing Wave Spectroscopy. *Food Hydrocolloids* **2009**, *23*, 1134–1138.
- (9) Hemar, Y.; Singh, H.; Horne, D. S. Determination of early stages of rennet-induced aggregation of casein micelles by diffusing wave spectroscopy and rheological measurements. *Curr. Appl. Phys.* **2004**, *4*, 362–365.
- (10) Cucheval, A. S. B.; Vincent, R. R.; Hemar, Y.; Otter, D.; Williams, M. A. K. Multiple particle tracking investigations of acid milk gels using tracer particles with designed surface chemistries and comparison with diffusing wave spectroscopy studies. *Langmuir* **2009**, *25*, 11827–11834.
- (11) Moschakis, T.; Murray, B. S.; Dickinson, E. On the kinetics of acid sodium caseinate gelation using particle tracking to probe the microrheology. *J. Colloid Interface Sci.* **2010**, *345*, 278–285.
- (12) Floury, J.; Madec, M. N.; Waharte, F.; Jeanson, S.; Lortal, S. First assessment of diffusion coefficients in model cheese by fluorescence recovery after photobleaching (FRAP). *Food Chem.* **2012**, *133*, 551–556.
- (13) Colsonet, R.; Soderman, O.; Mariette, F. Effect of casein concentration in suspensions and gels on poly(ethylene glycol)s NMR self-diffusion measurements. *Macromolecules* **2005**, *38*, 9171–9179.
- (14) Le Feunteun, S.; Mariette, F. Impact of casein gel microstructure on self-diffusion coefficient of molecular probes measured by H-1 PFG-NMR. *J. Agric. Food Chem.* **2007**, *55*, 10764–10772.
- (15) Le Feunteun, S.; Mariette, F. PFG-NMR techniques provide a new tool for continuous investigation of the evolution of the casein gel microstructure after renneting. *Macromolecules* **2008**, *41*, 2071–2078.
- (16) Le Feunteun, S.; Mariette, F. Effects of acidification with and without rennet on a concentrated casein system: A kinetic NMR probe diffusion study. *Macromolecules* **2008**, *41*, 2079–2086.
- (17) Le Feunteun, S.; Ouethrani, M.; Mariette, F. The rennet coagulation mechanisms of a concentrated casein suspension as observed by PFG-NMR diffusion measurements. *Food Hydrocolloids* **2012**, *27*, 456–463.
- (18) Salami, S.; Rondeau-Mouro, C.; van Duynhoven, J.; Mariette, F. PFG-NMR self-diffusion in casein dispersions: effects of probe size and protein aggregate size. *Food Hydrocolloids* **2013**, *31*, 248–255.
- (19) Wang, Y. J.; Therien-Aubin, H.; Baille, W. E.; Luo, J. T.; Zhu, X. X. Effect of molecular architecture on the self-diffusion of polymers in aqueous systems: A comparison of linear, star, and dendritic poly(ethylene glycol)s. *Polymer* **2010**, *51*, 2345–2350.

- (20) Loren, N.; Shtykova, L.; Kidman, S.; Jarvoll, P.; Nyden, M.; Hermansson, A.-M. Dendrimer diffusion in Kappa-Carrageenan gel structures. *Biomacromolecules* **2009**, *10*, 275–284.
- (21) Baille, W. E.; Malveau, C.; Zhu, X. X.; Kim, Y. H.; Ford, W. T. Self-diffusion of hydrophilic poly(propyleneimine) dendrimers in poly(vinyl alcohol) solutions and gels by pulsed field gradient NMR spectroscopy. *Macromolecules* **2003**, *36*, 839–847.
- (22) Bernin, D.; Goudappel, G.-J.; van Ruijven, M.; Altskar, A.; Strom, A.; Rudemo, M.; Hermansson, A.-M.; Nyden, M. Microstructure of polymer hydrogels studied by pulsed field gradient NMR diffusion and TEM methods. *Soft Matter* **2011**, *7*, 5711–5716.
- (23) Tomalia, D. A. Birth of a new macromolecular architecture: dendrimers as quantized building blocks for nanoscale synthetic polymer chemistry. *Prog. Polym. Sci.* **2005**, *30*, 294–324.
- (24) Dalgleish, D. G.; Spagnuolo, P.; Douglass Goff, H. A possible structure of the casein micelle based on high-resolution field-emission scanning electron microscopy. *Int. Dairy J.* **2004**, *14*, 1025–1031.
- (25) de Kruij, C. G. Supra-aggregates of casein micelles as a prelude to coagulation. *J. Dairy Sci.* **1998**, *81*, 3019–3028.
- (26) McMahon, D. J.; McManus, W. R. Rethinking casein micelle structure using electron microscopy. *J. Dairy Sci.* **1998**, *81*, 2985–2993.
- (27) Pitkowski, A. *Processus de gelification des caseines en presence de polyphosphates*; Universite de Maine: France, 2007.
- (28) Morris, G. A.; Foster, T. J.; Harding, S. E. Further observations on the size, shape, and hydration of casein micelles from novel analytical ultracentrifuge and capillary viscometry approaches. *Biomacromolecules* **2000**, *1*, 764–767.
- (29) de Gennes, P. G. Brownian motions of flexible polymer chains. *Nature* **1979**, *282*, 367–370.
- (30) Bouchoux, A.; Debbou, B.; Gesan-Guizieu, G.; Famelart, M. H.; Doublier, J. L.; Cabane, B. Rheology and phase behavior of dense casein micelle dispersions. *J. Chem. Phys.* **2009**, *131*, 165106–165111.
- (31) Matsukawa, S.; Ando, I. Study of self-diffusion of molecules in polymer gel by pulsed-gradient spin-echo  $^1\text{H}$  NMR. 3. Stearyl itocanamide/ $\text{N,N}$ -dimethylacrylamide copolymer gels. *Macromolecules* **1999**, *32*, 1865–1871.
- (32) Masaro, L.; Zhu, X. X. Interaction of ethylene glycol with poly(vinyl alcohol) in aqueous systems as studied by NMR spectroscopy. *Langmuir* **1999**, *15*, 8356–8360.
- (33) Möller, S. M.; Whittaker, A. K.; Stokes, J. R.; Gidley, M.; Andersen, U.; Bertram, H. C. Molecular water motions of skim milk powder solutions during acidification studied by  $(^{17}\text{O})$  and  $(^1\text{H})$  nuclear magnetic resonance and rheology. *J. Agric. Food Chem.* **2011**, *59*, 10097–10103.
- (34) Brosseau, C.; Guillermo, A.; Cohen-Addad, J. P. NMR observation of poly(ethylene oxide) dynamics in a poly(methyl methacrylate) matrix: effect of chain length variation. *Macromolecules* **1992**, *25*, 4535–4540.
- (35) Brereton, M. G.; Ward, I. M.; Boden, N.; Wright, P. Nature of the proton NMR transverse relaxation function of polyethylene melts. 1. Monodispersed polyethylenes. *Macromolecules* **1991**, *24*, 2068–2074.
- (36) Kimmich, R.; Roskopf, E.; Schnur, G.; Spohn, K. H. Chain dynamics and molecular weight dependence of carbon-13 and hydrogen-1 relaxation times in polystyrene and polyethylene melts. *Macromolecules* **1985**, *18*, 810–812.
- (37) Cohen Addad, J.-P.; Guillermo, A. Quantitative NMR characterization of long-range chain dynamics prior to reptation: Polyethylene-oxide. *Phys. Rev. Lett.* **2000**, *85*, 3432–3435.
- (38) Zoon, P.; Vanvliet, T.; Walstra, P. Rheological properties of rennet-induced skim milk gels. 1. Introduction. *Neth. Milk Dairy J.* **1988**, *42*, 249–269.
- (39) Karlsson, A. O.; Ipsen, R.; Ardo, Y. Rheological properties and microstructure during rennet induced coagulation of UF concentrated skim milk. *Int. Dairy J.* **2007**, *17*, 674–682.
- (40) Cooper, C.; Corredig, M.; Alexander, M. Investigation of the colloidal interactions at play in combined acidification and rennet of different heat-treated milks. *J. Agric. Food Chem.* **2010**, *58*, 4915–4922.
- (41) Anema, S. G.; Lee, S. K.; Klostermeyer, H. Rennet-induced aggregation of heated pH-adjusted skim milk. *J. Agric. Food Chem.* **2011**, *59*, 8413–8422.
- (42) Mellema, M.; Heesakkers, J. W. M.; van Opheusden, J. H. J.; van Vliet, T. Structure and scaling behavior of aging rennet-induced casein gels examined by confocal microscopy and permeametry. *Langmuir* **2000**, *16*, 6847–6854.
- (43) Lucey, J. A.; Tamehana, M.; Singh, H.; Munro, P. A. Effect of heat treatment on the physical properties of milk gels made with both rennet and acid. *Int. Dairy J.* **2001**, *11*, 559–565.
- (44) Lucey, J. A.; van Vliet, T.; Grolle, K.; Geurts, T.; Walstra, P. Properties of acid casein gels made by acidification with glucono- $\delta$ -lactone. 1. Rheological properties. *Int. Dairy J.* **1997**, *7*, 381–388.
- (45) Lucey, J. A.; Tamehana, M.; Singh, H.; Munro, P. A. Rheological properties of milk gels formed by a combination of rennet and glucono- $\delta$ -lactone. *J. Dairy Res.* **2000**, *67*, 415–427.
- (46) Walstra, P.; Vanvliet, T. The physical-chemistry of curd making. *Neth. Milk Dairy J.* **1986**, *40*, 241–259.
- (47) Sharma, S. K.; Mittal, G. S.; Hill, A. R. Effect of milk concentration, pH and temperature on Kappa-casein hydrolysis at aggregation, coagulation and curd cutting times of ultrafiltered milk. *Milchwissenschaft* **1994**, *49*, 450–453.
- (48) Mora-Gutierrez, A.; Farrell, H. M. J. Hydration of native and rennin-treated, cold-solubilized caprine caseins as determined by oxygen-17 nuclear magnetic resonance. *J. Dairy Sci.* **2001**, *84*, E93–E99.
- (49) Baldursdottir, S. G.; Kjoniksen, A. L.; Nystrom, B. The effect of riboflavin-photoinduced degradation of alginate matrices on the diffusion of poly(oxyethylene) probes in the polymer network. *Eur. Polym. J.* **2006**, *42*, 3050–3058.
- (50) Walther, B.; Loren, N.; Nyden, M.; Hermansson, A.-M. Influence of kappa-Carrageenan gel structures on the diffusion of probe molecules determined by transmission electron microscopy and NMR diffusometry. *Langmuir* **2006**, *22*, 8221–8228.
- (51) Colsenet, R.; Mariette, F.; Cambert, M. NMR relaxation and water self-diffusion studies in whey protein solutions and gels. *J. Agric. Food Chem.* **2005**, *53*, 6784–6790.
- (52) Babu, S.; Christophe Gimel, J.; Nicolai, T. Tracer diffusion in colloidal gels. *J. Phys. Chem. B* **2008**, *112*, 743–748.
- (53) Rollema, H. S.; Brinkhuis, J. A.; Vreeman, H. J. H-1-NMR studies of bovine kappa-casein and casein micelles. *Neth. Milk Dairy J.* **1988**, *42*, 233–248.